SEMARAK ILMU PUBLISHING
202103268166(003316878-P)

Journal of Advanced Research in Applied Mechanics

Journal homepage:
https://semarakilmu.com.my/journals/index.php/appl_mech/index
ISSN: 2289-7895

Influence of Laser Speed on the Area-Specific Resistance in Welded Stainless Steel for Solid Oxide Fuel Cell Interconnect

Mohd Faizal Tukimon[1], Hamimah Abd Rahman[1,*], Shahrin Hisham Amirnordin[1], Aiman Mohd Halil[2], Khairul Anuar Salleh[3], Tan Kang Huai[4], Zolhafizi Jaidi[1], Mohamed Abdelghani Elsayed Abdelghani Elshaikh[5]

1 Faculty of Mechanical and Manufacturing Engineering, Universiti Tun Hussein Onn Malaysia, 86400 Parit Raja, Batu Pahat, Johor, Malaysia
2 Faculty of Mechanical & Automotive Engineering Technology, Universiti Malaysia Pahang Al-Sultan Abdullah, 26600 Pekan, Pahang, Malaysia
3 Malaysian Nuclear Agency, Bangi, 43000 Kajang, Selangor, Malaysia
4 Centre for Advanced Materials, Faculty of Engineering and Technology, Tunku Abdul Rahman University of Management and Technology, Jalan Genting Kelang, 53300 Kuala Lumpur, Malaysia
5 Faculty of Mechanical Engineering, Islamic University of Madinah, Prince Naif Ibn Abdulaziz, Al Jamiah, Medina, Kingdom of Saudi Arabia

ARTICLE INFO

Article history:
Received 13 January 2025
Received in revised form 16 February 2025
Accepted 23 February 2025
Available online 30 March 2025

Keywords:
Solid oxide fuel cell; laser welding; stainless steel; interconnect; area specific resistance

ABSTRACT

The interconnect is one of the most important components in a solid oxide fuel cell (SOFC), as it is structurally and electrically connected to the stacked unit cells. One of the most important characteristics of an interconnect is that it must have a low area-specific resistance (ASR) to improve its electrical conductivity. In this study, welded ferritic stainless steel 430 (SS430) was fabricated by laser welding to analyse the ASR at different working temperatures. Digital microscope (DM) and electrochemical impedance (EIS) were used to study the structure of the process samples to investigate the welded area and ASR. The ASR was measured using C-V analysis via a two-point dual-probe technique at 400°C, 500°C, 600°C and 700°C. The results show that the ASR is lower in the middle part of the welded area than at the start and end areas of the welded parts. In addition, choosing the right range of laser speed played an important role in lowering the ASR. Therefore, a lower ASR is important for the SS430 to become an interconnect in SOFC.

1. Introduction

In an era of globalization, solid oxide fuel cells (SOFC) have become one of the promising technologies for generating clean, reusable, and renewable energy [1-5]. It is very well known that the SOFC has become an alternative way that is very sustainable and efficient as high as 70% in generating power compared to conventional power sources [6,7]. Figure 1 shows the efficiency of different types of fuel cells that have been investigated in previous studies. The efficiency of SOFC hinges on critical components, including the anode, cathode, electrolyte, and interconnect. The interconnect holds particular significance as it unites individual cells to form a fuel cell stack.

* *Corresponding author.*
E-mail address: hamimah@uthm.edu.my

https://doi.org/10.37934/aram.134.1.2534

Previously, according to Tukimon *et al.,* [8] and Cooper and Nigel [9] ceramic interconnects were prevalent in high-temperature fuel cell applications (750°C-1000°C). However, their fragility over prolonged operational periods raised concerns. It is reported by Yusof *et al.,* [10], that the operating temperature for low-temperature SOFC (LT-SOFC) is between 400°C and 600°C. The attention and approach in lowering the SOFC operational temperature has allowed the usage of stainless-steel interconnect as it can help to reduce material cost compared to the ceramic interconnect. As an alternative, the fabrication of ferritic stainless steel 430 (SS430) proves promising for SOFC interconnects due to its favorable attributes such as high electrical conductivity, low resistivity, ease of fabrication, and cost-effectiveness. Consequently, this study employs a laser welding process to explore the viability of SS430 as an interconnect material for SOFCs.

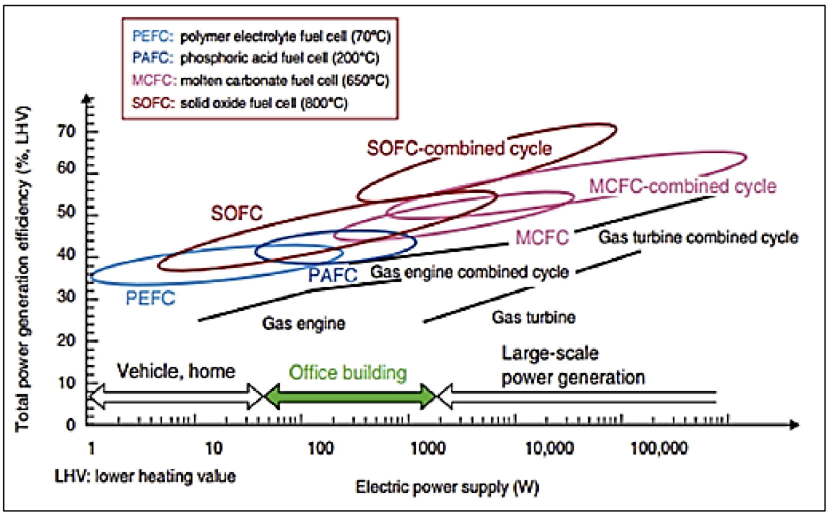

Fig. 1. Efficiency of SOFC with other fuel cell technologies [6]

Laser welding is an effective method for connecting or joining two or more materials. This technique has been broadly applied in the manufacturing industry owing to its advantages, such as extra production, automotive works, and the formation of a good quality weld with small heat-affected zones has been mentioned by Kovacs [11]. Particularly, Jamaludin *et al.,* [12] state that industries that use laser welding are found to effectively produce critical components such as batteries and fuel cells, leading to a huge increase in fabrication. Nevertheless, some problems need to be resolved regarding the laser welding parameter in the application of SOFC interconnect. Therefore, a good laser welding parameter needs to be investigated to improve the joining in SOFC interconnect.

Morphology analysis of welded stainless steel is important for investigating the defects that exist inside the welded area. Previous data produced by Chen *et al*., [13] indicate that a circular or stirring effect on the laser changes the solidification rate on the welded area, resulting in improved morphology and reduced deformation of the welded area. Figure 2 illustrates a typical instance of welding defects that may arise post the joining procedure. The existence of these defects has impacted the characteristics of the welded material. In the context of SOFC, defects like porosities and incomplete penetration have the potential to result in gas and water leakage during operation, adversely affecting the efficiency of SOFC performance. Consequently, there is a necessity to investigate laser welding parameters for minimizing, and ideally eliminating, the occurrence of such defects.

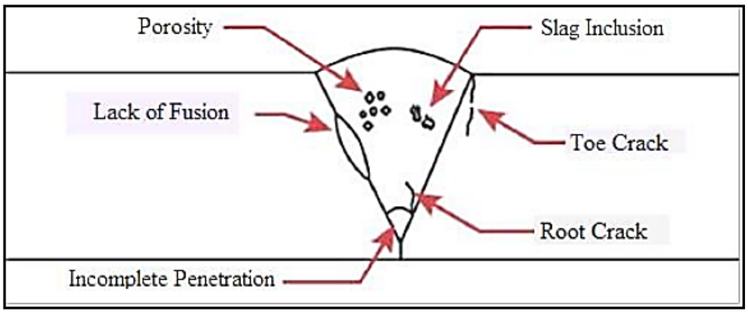

Fig. 2. Types of defects after the laser welding process [8]

Other than the morphology, the analysis of the area-specific resistance (ASR) is important in the process of design and evaluation of SOFC interconnect since it is related to the electrical resistivity experienced by a unit area of the interconnect during operation. Besides, it acts as a performance metric for fuel cells, allowing researchers to evaluate the efficiency of energy conversion. Next, ASR measurements serve as a diagnostic tool, identifying issues or anomalies within the cell, and guiding maintenance and optimization. Furthermore, ASR data is essential for material optimization, providing insights into the impact of different materials on performance, aiding in electrode and electrolyte characterization, and contributing to efficiency improvement through targeted modifications. Therefore, the ASR measurements also play a role in quality control during manufacturing, validate theoretical models, and advance fuel cell technology by uncovering fundamental mechanisms for ongoing development and improvement.

In this study, the focus on investigating the structure and the ASR of the SOFC interconnect has been conducted, specifically through fabricating the interconnect material by using laser welding.

2. Methodology

For the laser welding process, stainless steel grade 430 (SS430) with a thickness of 0.1 mm is used for the application of SOFC interconnect. The chemical configuration of the SS430 is shown in Table 1. The specimens were cut to 60mm x 60mm dimensions and then cleaned by using ethanol to make sure there was no dirt or contamination on the surface of the base material. By stacking two thin SS430, the laser welding process has been conducted based on Figure 3. The specification of the laser welding machine can be obtained from previous studies [12,14,15]. The preliminary testing for the laser welding process has been done and the parameter that has achieved joining the two stacks of stainless steel with 0.1 mm thickness is shown in Table 2.

After the laser welding process, the analysis of the surface-welded area has been conducted through the utilization of a Digital Microscope (DM). This microscopic examination allows for a detailed inspection of the structural characteristics of the welded stainless steel in the SOFC interconnects. The analysis captures high-resolution images, enabling a thorough investigation of the weld quality and potential defects such as porosity and cracks. This analysis plays a crucial role in understanding the influence of laser welding parameters on the surface properties of the welded region. By scrutinizing the structural features, it becomes possible to optimize welding parameters for improved resistivity of the stainless-steel interconnects in SOFC.

Table 1
Chemical configuration of SS430

Element	C	SI	Mn	P	S	Cr	Fe
Wt%	1.97	0.46	0.59	0.09	0.05	15.87	80.99

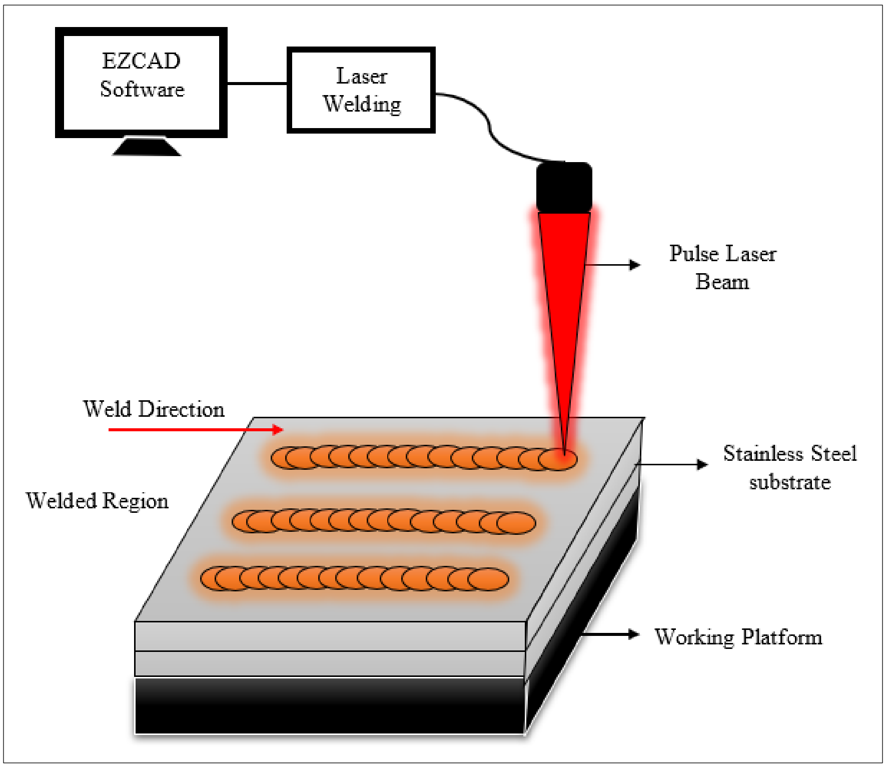

Fig. 3. The schematic drawing of the laser welding process

Table 2
Parameter of the laser welding process

Sample	Laser power (%)	Laser speed (mms^{-1})
1	100.0	50.0
2	100.0	40.0
3	100.0	30.0

As for the ASR determination, Current Voltage (I-V) testing from an electrochemical impedance (EIS) machine is then conducted. Using a two-point dual-probe technique which connected the EIS machine with the direct current (DC) flow to the sample, the ASR is gathered at different working temperatures after 30 minutes of the soaking phase. The specimen is cut into a 1.3 cm x 0.3 cm and then sandwiched in between the platinum mesh (Pt-mesh) that is connected to the dual probe connector. The schematic of the experimental setup is shown in Figure 4.

As shown in Figure 4, the welded sample is sandwiched using a Pt-mesh to let the current flow in the samples. The resistance is obtained from the gradient of the I-V graph which is from DC input (100mA to 10mA). The value of ASR can be calculated through Eq. (1) which is:

$$ASR = \frac{1}{2}\left(\frac{1}{\rho} \cdot A\right) \tag{1}$$

where $1/\rho$ is the gradient of the graph from I-V analysis, whereas A is the active area of the sample. In this case, the area of each sample is fixed. The ASR was determined at the operating temperatures of 700°C, 600°C, 500°C and 400°C and analyzed with NOVA Autolab Software version 1.11 and calculated using Eq. (1) following Ohm's Law mentioned by Tan *et al.*, [16].

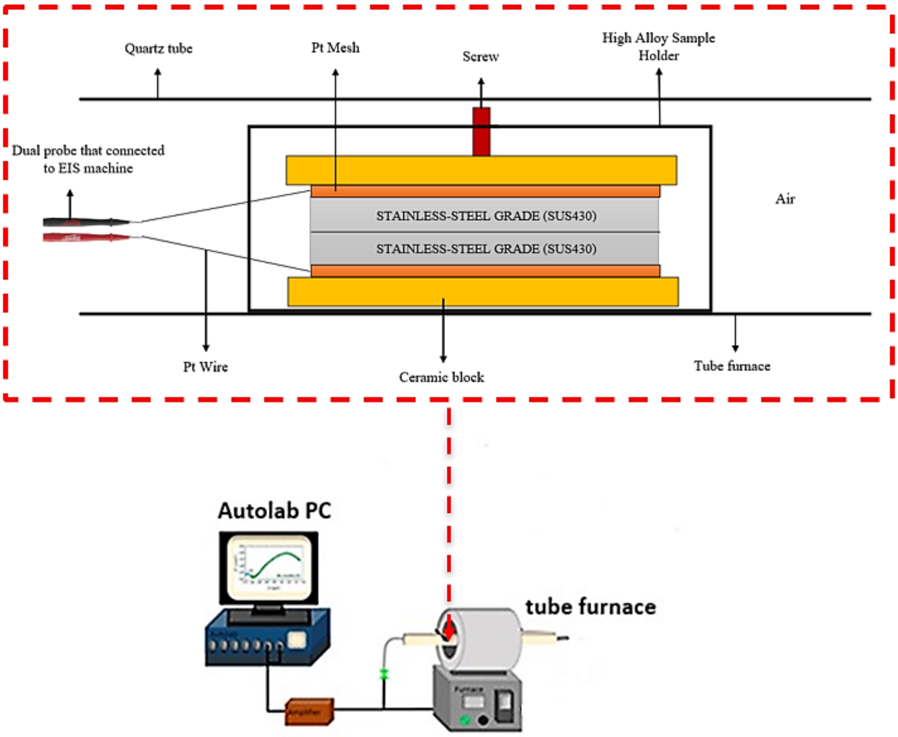

Fig. 4. Experimental setup for the determination of ASR

3. Results

3.1 Surface Welded Structure

During the laser welding process of two stacks of FSS, distinct heat patterns was observed. Initially, as the heat gradually increased, it melted the structure of the FSS. At this stage, the joining was not effectively connected. As the process continued, the heat reached stability at the middle point of the welded area, allowing for the joining of the FSS. However, towards the end of the welded area, the heat has already overheated toward the sample. This led to faster liquidation and solidification of the samples, resulting in a well-joined structure with additional reinforcement. Hence, the quality of the welded part is recognized in the middle part of the welded area.

The welded area of each sample has been shown in Table 3. This welded area joins two plates of SS430 by using different laser welding parameters shown in Table 2. Three samples have been fabricated using different laser speeds to observe the effect of laser speed on the welded structure.

From the laser welding processing, all samples showed no visible porosity or defect which indicates the chosen parameter is acceptable in joining two stacks of SS430. The width of the welded seams is approximately ±1.0 mm. As we can see from Table 3, the texture of the surface welded area at a welding speed of 50 mms^{-1} is smoother compared to 40 and 30 mms^{-1} welding speeds. A higher welding speed usually makes the solidification, and cooling rates increase, potentially resulting in a fine-grained and smoother surface welded area [17-19]. Meanwhile, a slower welding speed has allowed the increase of heat input from the laser to the base material which leads to a rougher surface texture. Also, the welded contrast at slower welding speed is darker in comparison with higher welding speed. This shows that the heat input at a slower welding speed is higher than the higher welding speed.

Table 3
Surface structure using digital microscopy (DM) with 150X magnification

Sample	The surface of the welded area	Colour distribution on the welded area
Sample 1 (LP100 LS50)	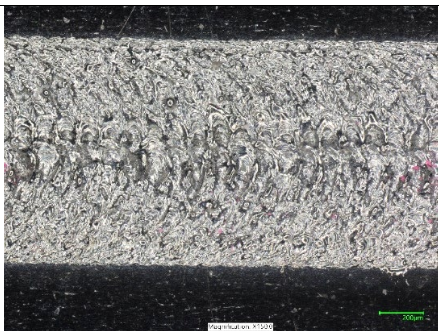	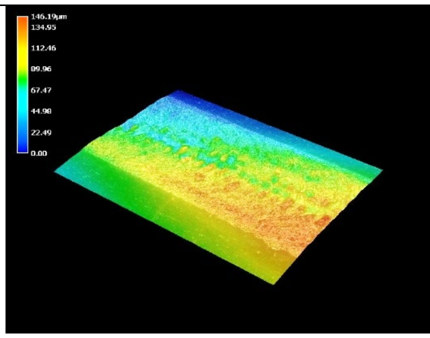
Sample 2 (LP100 LS40)	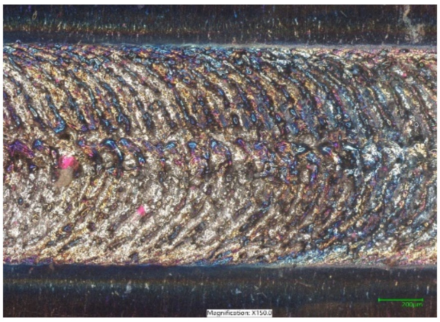	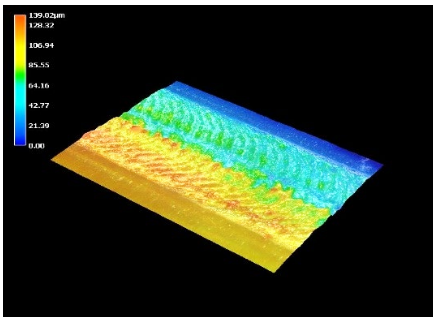
Sample 3 (LP100 LS30)	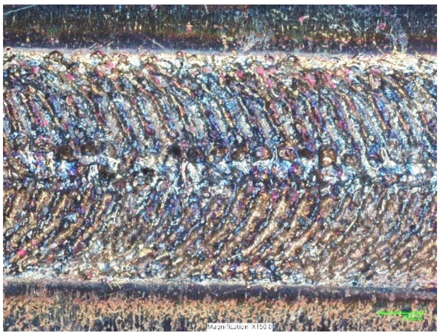	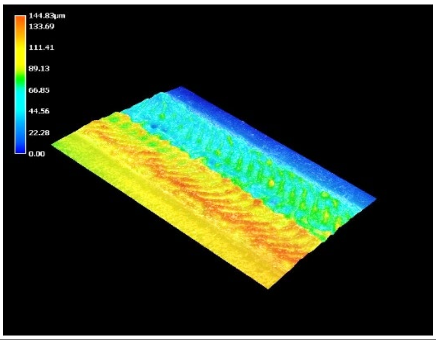

To obtain a more comprehensive understanding of the surface-welded structure, a colour distribution map has been generated based on the Digital Microscope (DM) analysis. The colour representation aids in visualizing the structural variations across the welded area. Notably, the blue areas signify that the structure of the welded region aligns with the level of the base material, while the transition from green and red indicates a reinforced structure in the welded area. Conversely, at the blue zones overlapped with green or red zones, showing the presence of welding sag in those areas as known as underfill [20-22]. The maximum depth of welding sag has also been generated through the DM analysis, and the results are presented in Table 4.

Table 4 indicates a notable rise in the maximum sagging depth from Sample 1 to Sample 3. This observation suggests a correlation between the increased welding speed and the amplified sagging depth. Thus, a thorough examination of welding parameters is essential to gain insights into their impact on the surface quality and, consequently, the performance of the welded components. Therefore, the investigation of this parameter in laser welding is crucial for ensuring the achievement of desired welded quality and identifying the operating parameters that enhance surface characteristics.

Table 4
Maximum sagging depth on the welded area

Sample	Sagging depth (µm)
1	29.12
2	35.32
3	42.57

3.2 Area-Specific Resistance

The area-specific resistance (ASR) in welded ferritic stainless steel is often influenced by various factors such as changes in welded structure and potential contamination during the welding process. Regarding the ASR, an examination was conducted at three distinct sections of the welded area, namely the start, middle, and end. The ASR results for Sample 1, Sample 2, and Sample 3 have been visually represented through bar graphs, as depicted in Figures 5, 6, and 7, respectively.

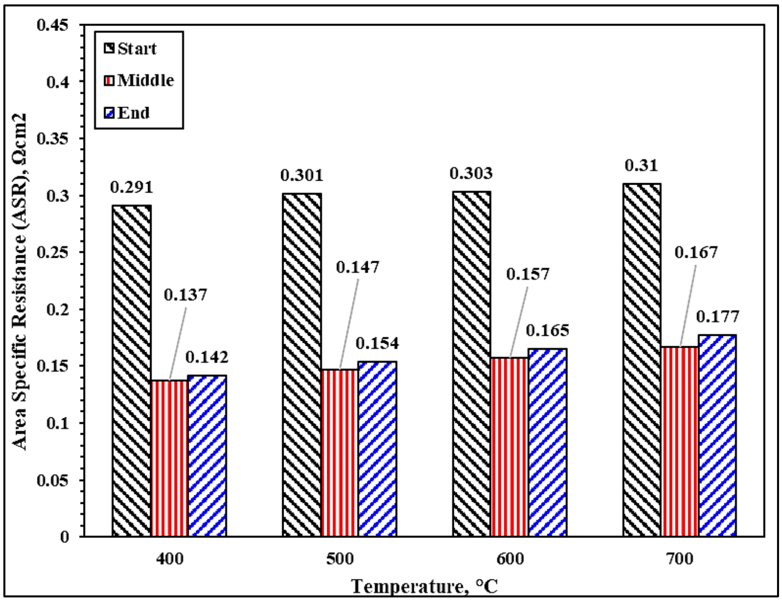

Fig. 5. ASR Vs temperature for Sample 1

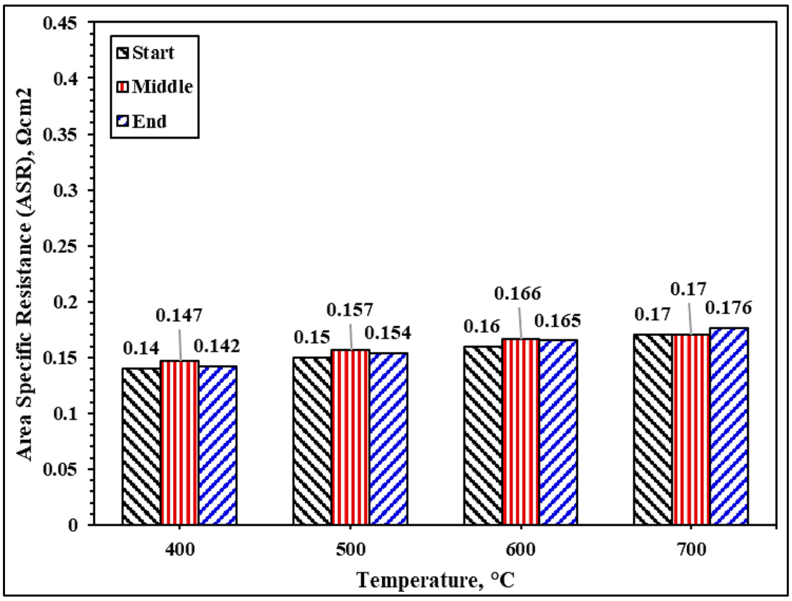

Fig. 6. ASR Vs temperature for Sample 2

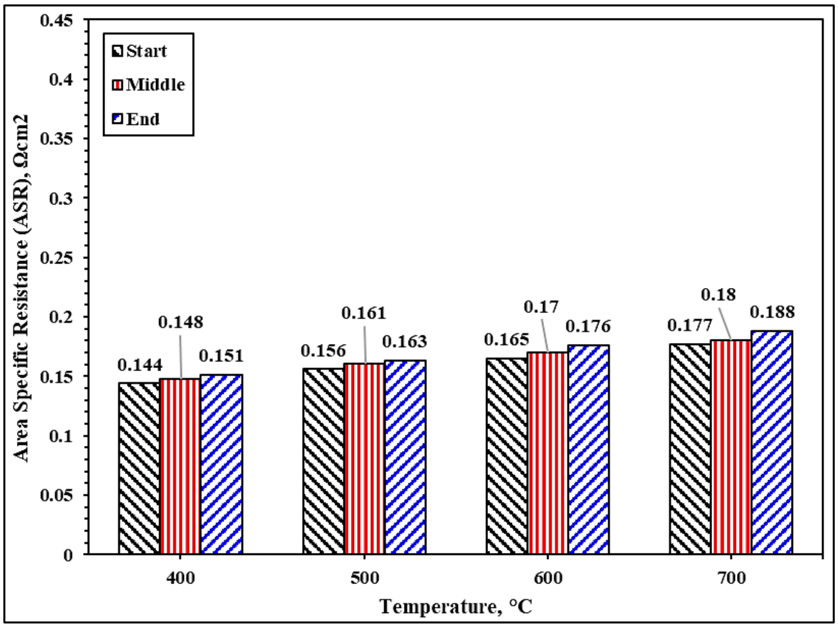

Fig. 7. ASR Vs temperature for Sample 3

From the plotted graph, it is evident that the trend remains consistent across all samples. Nevertheless, in the case of Sample 1, there is an abnormal peak that is observed at the beginning of the welded area for each temperature. The ASR demonstrates an increase with rising temperatures, ranging from 0.29 Ωcm^2 to 0.31 Ωcm^2. The rise in ASR indicates the existence of reinforcement at the surface of the welded area during the welding process, causing a hindrance to the electron flow within the welded region. Hence, the disturbance of the electron flow has reduced the efficiency of electrical energy generation in SOFC systems.

As for Sample 2 and Sample 3, the range of ASR is almost the same which is approximately from 0.14 Ωcm^2 to 0.19 Ωcm^2. It is mentioned by Tan *et al.,* [23] that the range of ASR for uncoated stainless steel is between 0.124 Ωcm^2 and 0.241 Ωcm^2. From these data, we can see that as the welding speed is lowered, the value of ASR decreases. The acceptable ASR value for ferritic stainless-steel interconnects in SOFC applications can vary based on specific system requirements and design considerations. Therefore, getting a lower ASR value is desirable as it indicates lower resistivity with better electrical conductivity and, consequently, improved performance of the SOFC system.

4. Conclusions

As for the conclusion, the effect of the welding speed that has affected the welded structure and ASR has been studied. From this investigation, it is found that the laser welding parameter which is laser power (100%) with laser speed (30 mms^{-1}, 40 mms^{-1}, and 50 mms^{-1}) is suitable for joining two thin ferritic stainless steel. As the welding speed increases, the surface welded area is smoother in comparison with slower welding speed. Besides, the sample that has a higher welding speed also gives the lowest welding sag compared to the other samples. The value of ASR needs to be as low as possible to increase the effectiveness of the electron flow for generating electrical energy in the SOFC system. It is recommended that the investigation of the parameter of laser welding needs to be optimized to achieve a well-defined and ensure the desired welded quality and increase the performance of the welded components.

Acknowledgement
The research was supported by Universiti Tun Hussein Onn Malaysia (UTHM) through RE-GG Vot H879.

References

[1] Hussain, Saddam, and Li Yangping. "Review of solid oxide fuel cell materials: Cathode, anode, and electrolyte." *Energy Transitions* 4, no. 2 (2020): 113-126. https://doi.org/10.1007/s41825-020-00029-8
[2] Alaedini, Amir Hossein, Haniyeh Kazemi Tourani, and Majid Saidi. "A review of waste-to-hydrogen conversion technologies for solid oxide fuel cell (SOFC) applications: Aspect of gasification process and catalyst development." *Journal of Environmental Management* 329 (2023): 117077. https://doi.org/10.1016/j.jenvman.2022.117077
[3] Biswas, Saheli, Dattatray S. Dhawale, Tara Hosseini, Gurpreet Kaur, Sarbjit Giddey, and Nawshad Haque. "A review on critical metals used in solid oxide cells for power↔ X applications and materials recyclability." *ACS Sustainable Chemistry & Engineering* 12, no. 16 (2024): 6037-6058. https://doi.org/10.1021/acssuschemeng.3c07934
[4] Udomsilp, David, Jürgen Rechberger, Raphael Neubauer, Cornelia Bischof, Florian Thaler, Wolfgang Schafbauer, Norbert H. Menzler, Lambertus G.J. de Haart, Andreas Nenning, Alexander K. Opitz, Olivier Guillon, Martin Bram "Metal-supported solid oxide fuel cells with exceptionally high power density for range extender systems." *Cell Reports Physical Science* 1, no. 6 (2020). https://doi.org/10.1016/j.xcrp.2020.100072
[5] Singh, Mandeep, Dario Zappa, and Elisabetta Comini. "Solid oxide fuel cell: Decade of progress, future perspectives and challenges." *International Journal of Hydrogen Energy* 46, no. 54 (2021): 27643-27674. https://doi.org/10.1016/j.ijhydene.2021.06.020
[6] Tan, K. H., H. A. Rahman, and H. Taib. "Ba0. 5Sr0. 5Co0. 8Fe0. 2O3− δ-Sm0. 2Ce0. 8O1. 9 carbonate perovskite coating on ferritic stainless steel interconnect for low temperature solid oxide fuel cells." *Materials Chemistry and Physics* 254 (2020): 123433. https://doi.org/10.1016/j.matchemphys.2020.123433
[7] Ahmad, Muhammad Zaid, Sahrim Haji Ahmad, Ruey Shan Chen, Aznan Fazli Ismail, Roshasnorlyza Hazan, and Nurul Akidah Baharuddin. "Review on recent advancement in cathode material for lower and intermediate temperature solid oxide fuel cells application." *International Journal of Hydrogen Energy* 47, no. 2 (2022): 1103-1120. https://doi.org/10.1016/j.ijhydene.2021.10.094
[8] Tukimon, Mohd Faizal, Shahrin Hisham Amirnordin, Umira Asyikin Yusop, Zolhafizi Jaidi, Azzura Ismail, and Sufizar Ahmad. "Important parameters of laser welding for metallic materials interconnect in fuel cell: a short review." *Malaysian Journal of Microscopy* 18, no. 1 (2022): 158-176.
[9] Cooper, Samuel J., and Nigel P. Brandon. "An introduction to solid oxide fuel cell materials, technology and applications." In *Solid Oxide Fuel Cell Lifetime and Reliability*, pp. 1-18. Academic Press, 2017. https://doi.org/10.1016/B978-0-08-101102-7.00001-5
[10] Yusop, Umira Asyikin, Tan Kang Huai, Hamimah Abdul Rahman, Nurul Akidah Baharuddin, and Jarot Raharjo. "Electrochemical performance of barium strontium cobalt ferrite-samarium doped ceria-argentum for low temperature solid oxide fuel cell." In *Materials Science Forum*, vol. 991, p. 94-100. Trans Tech Publications Ltd, 2020. https://doi.org/10.4028/www.scientific.net/MSF.991.94
[11] Kovacs, Tunde. "Laser welding process specification base on welding theories." *Procedia Manufacturing* 22 (2018): 147-153. https://doi.org/10.1016/j.promfg.2018.03.023
[12] Jamaludin, M. N., M. M. Quazi, M. H. Aiman, and M. Ishak. "Distortion in laser micro welding of stainless steel SS304 foils." *Materials Today: Proceedings* 109 (2024): 81-86. https://doi.org/10.1016/j.matpr.2023.10.053
[13] Chen, Cong, Haipeng Zhou, Changjian Wang, Lili Liu, Yuhui Zhang, and Ke Zhang. "Laser welding of ultra-high strength steel with different oscillating modes." *Journal of Manufacturing Processes* 68 (2021): 761-769. https://doi.org/10.1016/j.jmapro.2021.06.004
[14] Linggamm, R., M. M. Quazi, M. Nasir Bashir, M. Ishak, and M. H. Aiman. "The influence of nanosecond fibre laser on the removal of paint on metallic surface." *International Journal of Technology & Engineering Studies* 7, no. 2 (2021). https://doi.org/10.20469/ijtes.7.10001-2
[15] Zul, M. H., Mahadzir Ishak, M. H. Aiman, and M. M. Quazi. "Influence of laser power in nanosecond laser texturing for a hydrophobic state on SS316L." *Journal of Mechanical Engineering and Sciences* 15, no. 4 (2021): 8592-8600. https://doi.org/10.15282/jmes.15.4.2021.11.0677
[16] Tan, K. H., H. A. Rahman, and H. Taib. "Ba0. 5Sr0. 5Co0. 8Fe0. 2O3− δ-Sm0. 2Ce0. 8O1. 9 carbonate perovskite coating on ferritic stainless steel interconnect for low temperature solid oxide fuel cells." *Materials Chemistry and Physics* 254 (2020): 123433. https://doi.org/10.1016/j.matchemphys.2020.123433

[17] Li, Junzhao, Qingjie Sun, Yibo Liu, Zuyang Zhen, Qi Sun, and Jicai Feng. "Melt flow and microstructural characteristics in beam oscillation superimposed laser welding of 304 stainless steel." *Journal of Manufacturing Processes* 50 (2020): 629-637.https://doi.org/10.1016/j.jmapro.2019.12.053

[18] Bhatt, Dhruv, and Ashish Goyal. "Effect of parameters of Nd YAG laser welding on AISI 316 Stainless steel and Brass." In *IOP Conference Series: Materials Science and Engineering*, vol. 455, no. 1, p. 012118. IOP Publishing, 2018. https://doi.org/10.1088/1757-899X/455/1/012118

[19] Nguyen, Quyen, Alireza Azadkhou, Mohammad Akbari, Afshin Panjehpour, and Arash Karimipour. "Experimental investigation of temperature field and fusion zone microstructure in dissimilar pulsed laser welding of austenitic stainless steel and copper." *Journal of Manufacturing Processes* 56 (2020): 206-215. https://doi.org/10.1016/j.jmapro.2020.03.037

[20] Salleh, Muhammad Naqiuddin Mat, Mahadzir Ishak, Kazuhiko Yamasaki, Moinuddin Mohammed Quazi, and Aiman Mohd Halil. "Pulsed Nd: YAG laser parameters effect on welding uncoated advance high strength steel (AHSS) for automotive." *J Adv Res Fluid Mech Therm Sci* 84, no. 1 (2021): 91-100.https://doi.org/10.37934/arfmts.84.1.91100

[21] Quazi, M. M. "An overview of laser welding of high strength steels for automotive application." *KA Manoharan, MM Quazi, MN Bashir, MNM Salleh, AQ Zafiuddin, and R. Linggamm,"An Overview of Laser Welding of High Strength Steels for Automotive Application", International Journal of Technology and Engineering Studies* 6, no. 1 (2020): 23-40. https://doi.org/10.20469/ijtes.6.10004-1

[22] You, D. Y., X. D. Gao, and S. Katayama. "Review of laser welding monitoring." *Science and Technology of Welding and Joining* 19, no. 3 (2014): 181-201.https://doi.org/10.1179/1362171813Y.0000000180

[23] Tan, K. H., Hamimah Abd Rahman, and Hariati Taib. "Coating layer and influence of transition metal for ferritic stainless steel interconnector solid oxide fuel cell: A review." *International Journal of Hydrogen Energy* 44, no. 58 (2019): 30591-30605. https://doi.org/10.1016/j.ijhydene.2019.06.155